Fast crystallization below the glass transition temperature in hyperquenched systems

Pierre Lucas^{1,*}, Wataru Takeda¹, Julian Pries², Julia Benke-Jacob², Matthias Wuttig^{2,3}

* Corresponding author: Pierre@arizona.edu

Abstract: Many phase change materials (PCMs) are found to crystallize without exhibiting a glass transition endotherm upon reheating. In this paper we review experimental evidence revealing that these PCMs and likely other hyperquenched molecular and metallic systems can crystallize from the glassy state when reheated at standard rate. Among these evidences, PCMs annealed below the glass transition temperature $T_{\rm g}$ exhibit slower crystallization kinetics despite an increase in number of sub-critical nuclei that should promote crystallization speed. Flash calorimetry uncovers the glass transition endotherm hidden by crystallization and reveals a distinct change in kinetics when crystallization switches from the glassy to the supercooled liquid state. The resulting $T_{\rm g}$ value also rationalizes the presence of the pre- $T_{\rm g}$ relaxation exotherm ubiquitous of hyperquenched systems. Finally, the shift in crystallization temperature during annealing exhibit a non-exponential decay that is characteristic of structural relaxation in glass. Modeling using a modified Turnbull equation for nucleation rate supports the existence of sub- $T_{\rm g}$ fast crystallization and emphasizes the benefit of a fragile-to-strong transition for PCM applications due to a reduction in crystallization at low temperature (improved data retention) and increasing its speed at high temperature (faster computing).

Introduction:

Crystallization below the glass transition temperature $T_{\rm g}$ is normally extremely slow due to the kinetically arrested atomic mobility in this temperature range¹. While oxide glasses mainly obey this behavior, organic glasses commonly exhibit unusually high crystallization rates below $T_{\rm g}^{2-9}$. This behavior results from a decoupling between crystallization rates and viscous flow caused by interfacial effects. Hikima *et al.*² observed anomalously high crystallization rates in the glass transition region of o-terphenyl and assigned it to an enhancement of homogeneous nucleation at the liquid-crystal interface. A similar process was observed by Ishida *et al.* in nifedipine³. Schammé *et al.* assigned the crystallization of ball-milled quinidine amorphous powders to high molecular mobility on the surface of amorphous grains⁴. Willart *et al.* observed an identical effect in griseofulvin⁵. Yu *et al.* also observed fast surface crystallization and glass-crystal

¹ Department of Materials Science and Engineering, University of Arizona, Tucson, AZ 85712, United States

² Institute of Physics IA, RWTH Aachen University, 52074 Aachen, Germany

³ Peter Grünberg Institute (PGI 10), Forschungszentrum Jülich, 52428 Jülich, Germany

growth in several organic compounds⁶⁻⁹. But while the crystallization rate of these systems is abnormally high in the region directly below $T_{\rm g}$ due to a decoupling from viscosity, they are relatively good glass formers and all exhibit a clear calorimetric glass transition. Instead, an increasing number of rapidly quenched systems have been found to crystallize prior to exhibiting a calorimetric glass transition: this includes water^{10,11}, metallic glasses^{12,13} and phase change materials (PCMs)¹⁴⁻¹⁶. In these systems, rapid crystallization occurs at temperatures up to 50 °C below $T_{\rm g}$ where diffusive processes would normally be exceedingly slow. The inability to observe a clear glass transition has in some cases led to controversies such as in the case of water^{10,17,18}. Here we review experimental evidences indicating that fast sub- $T_{\rm g}$ crystallization occurs in many amorphous PCMs. We then use the Turnbull method to explain the phenomenon and its relation to fragility.

Sub- T_g crystallization in PCMs:

PCMs exhibit a range of crystallization behavior depending on their composition¹⁹. Prominent PCMs such as $Ge_2Sb_2Te_5$, AIST ($Ag_4In_3Sb_{67}Te_{26}$) or GeTe all crystallize without prior glass transition endotherms when reheated at conventional rates (~20 °C/min)¹⁴⁻¹⁶. Other PCMs such as $Ge_3Sb_6Te_5$ exhibit a clear glass transition prior to crystallization²⁰. Figure 1 compares the excess heat capacity C_p^{exc} of as-deposited GeTe and $Ge_3Sb_6Te_5$ during a heating ramp at a rate of 40 °C/min. The comparison of these two glasses is insightful because they have nearly identical T_g values i.e. T_g =190 °C for $GeTe^{16}$ and T_g =193 °C for $Ge_3Sb_6Te_5^{20}$ but exhibit distinct crystallization behavior. The first feature on the thermogram of Figure 1 is an exotherm starting near 100 °C which is characteristic of hyperquenched systems trapped in a high fictive temperature state²¹. During reheating at slow rate both glasses release enthalpy as they dynamically relax towards the metastable supercooled liquid state. $Ge_3Sb_6Te_5$ eventually exhibits a glass transition endotherm near 193 °C prior to crystallization near 230 °C. In contrast, GeTe starts to crystallize as it is still relaxing tens of degrees below T_g . This strongly suggests that GeTe (and other PCMs) crystallize from the glassy state instead of the supercooled liquid state above T_g .

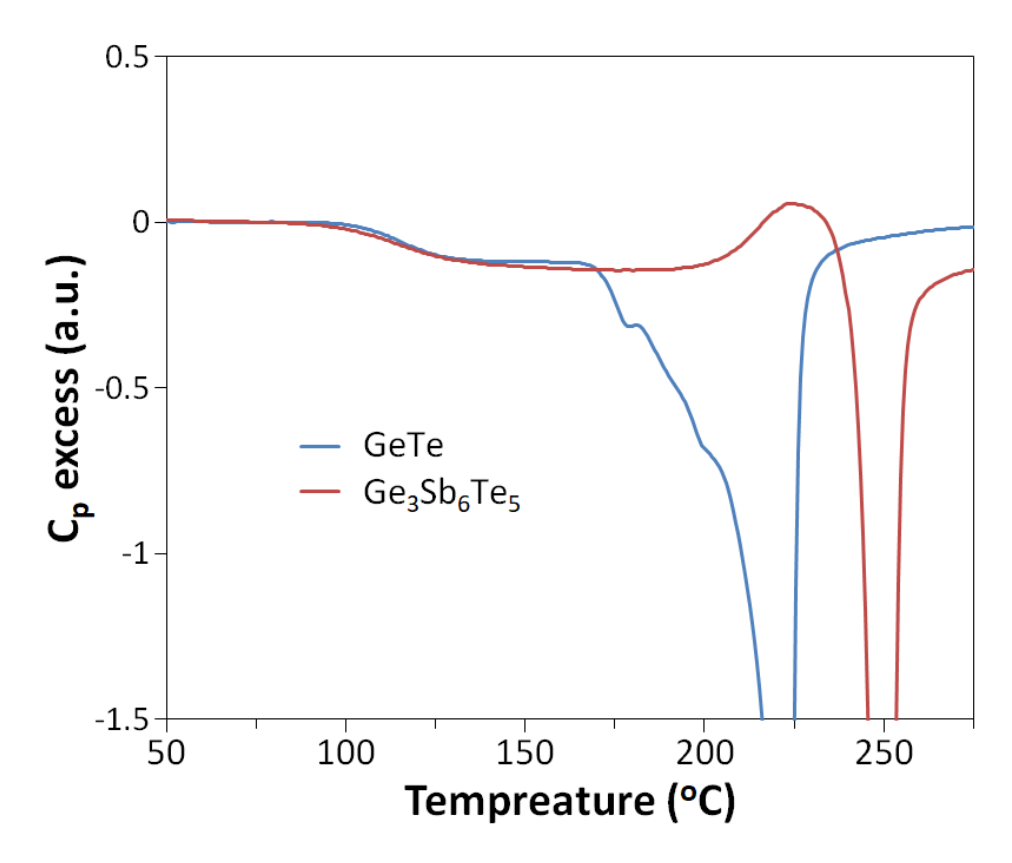


Figure 1: Excess heat capacity C_p^{exc} of as-deposited GeTe and Ge₃Sb₆Te₅ during a heating ramp at a rate of 40 °C/min. (Data from Ref. [16,20])

The absence of a clear calorimetric glass transition endotherm in some PCMs have led to a broad range of reported $T_{\rm g}$ values spanning in some cases over 100 °C²²⁻²⁶. For example $T_{\rm g}$ values for Ge₂Sb₂Te₅ have been reported from 100 °C²² to 200 °C²⁶ and that of AIST from 105 °C²⁷ to 182 °C¹⁵. However, the T_g of PCMs can also be estimated from their relaxation exotherm using the Velikov et al. method¹¹ as shown in Figure 2. It is found that hyperquenched glasses spanning many categories of compositions (metallic, oxides, covalent, organic), a broad range of fragility (m=17 to 81) and a broad range of T_g (-30 °C to 670 °C) all obey a similar pattern of exothermic relaxation when reheated at slow rate. All systems exhibit a maximum in relaxation of trapped enthalpy near $T/T_g \approx 0.9$. This provides an alternative mean of estimating T_g for controversial PCMs such as Ge₂Sb₂Te₅. A T_g assignment of 200 °C for Ge₂Sb₂Te₅ shows a relaxation behavior consistent with all systems and in particular with that $Ge_3Sb_6Te_5$ where T_g is unambiguously known. Instead, a $T_{\rm g}$ assignment of 110 °C indicates a glass that would undergo a maximum of relaxation at a temperature above T_g when the system has already reached the supercooled liquid. This outcome is not sound since there would be no driving force for relaxation in the metastable supercooled liquid state. The $T_{\rm g}$ must therefore lay at higher values. The same pattern is observed for GeTe with a T_g =193 °C and AIST with a T_g =182.5 °C In turn, this indicates that these PCMs indeed crystallize below $T_{\rm g}$ as previously reported ¹⁴⁻¹⁶.

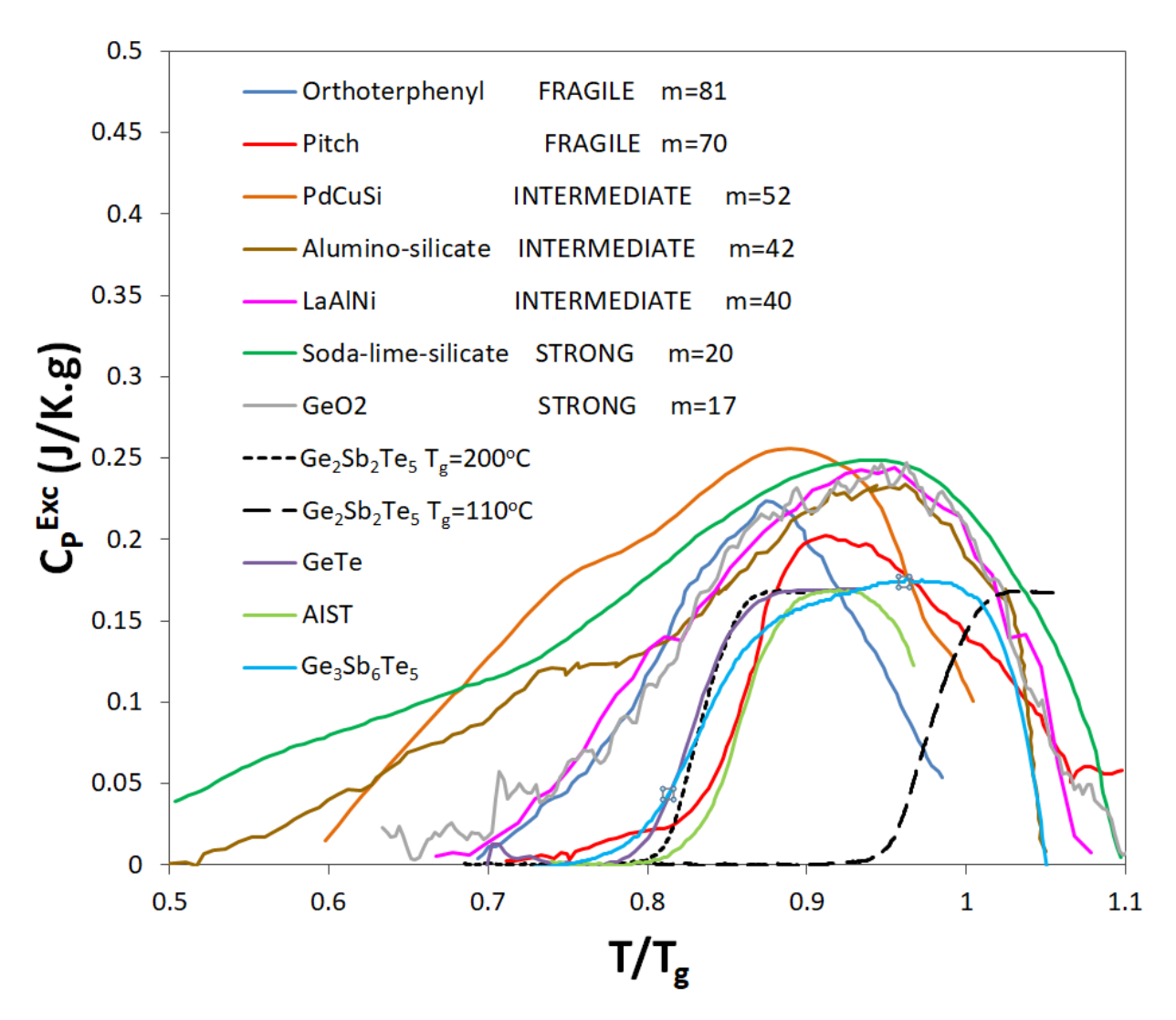


Figure 2: Enthalpy recovery exotherm for a wide variety of hyperquenched glasses including oxide, metallic and molecular glasses over a broad range of T_g (–30 °C to 670 °C) and a broad range of fragility (m = 17 to 81). Orthoterphenyl ¹¹, Pitch ²⁸, Pd_{77.5}Cu₆Si_{16.5} ²⁹, La₅₅Al₂₅Ni₂₀ ³⁰, Basaltic fiber (SiO₂ 49.3 Al₂O₃ TiO₂ 1.8 FeO 11.7 CaO 10.4 MgO 3.9 Na₂O 3.9 K₂O 0.7) ³¹, soda-lime-silicate (SiO₂ 70.5 Na₂O 8.7 K₂O 7.7 CaO 11.6 Sb₂O₃ 1.1 SO₃ 0.2) ³², GeO₂ ³³. All glasses show the onset of relaxation of trapped enthalpy near T/T_g ≈0.5–0.7 and a maximum of relaxation near T/T_g ≈0.9. Comparison of these exotherms with that of phase change materials using Velikov's excess heat capacity method¹¹ indicates that the standard T_g value for Ge₂Sb₂Te₅ is ~200 °C.

Further evidence for sub- $T_{\rm g}$ crystallization in PCMs can be garnered through the use of flash differential scanning calorimetry (FDSC)^{14,15}. As shown long ago by Henderson³⁴, application of the Kissinger method³⁵ to crystallization kinetics indicate that the temperature of a crystallization exotherm maximum $T_{\rm P}$ is a function of heating rate due to the kinetic barrier for crystal growth in supercooled liquid. Specifically, higher heating rates permit to delay the crystallization event to

higher temperatures. The use of FDSC should then permit to notably raise the onset of the crystallization exotherm. This offers a strategy to uncover the glass transition endotherm that is hidden by crystallization at standard heating rates. Figure 3(a) shows the thermograms obtained from heating as-deposited Ge₂Sb₂Te₅ at rates ranging from 50 K/s to 30,000 K/s. At slower rates the relaxation exotherm is present prior to crystallization along with the evolution of the socalled "shadow-glass transition" 18. At sufficiently high rates near 10,000 K/s the relaxation exotherm vanishes and reveals a glass transition endotherm prior to crystallization. This indicates that the crystallization now takes place from the undercooled liquid rather than the glassy state. If this is the case, the crystallization kinetics should be notably different. The activation energy for crystallization can be obtained through construction of a Kissinger plot as shown in Figure 3(b). The Kissinger plot of Ge₂Sb₂Te₅ shows a sudden change in crystallization activation energy from 3.13 eV (blue markers) to 0.69 eV (red markers) that is concomitant with the switch in crystallization from the glassy state to the supercooled liquid state (Figure 3(a))14. This switch in kinetic behavior was observed for both AIST¹⁵ and Ge₂Sb₂Te₅¹⁴. While the activation energy should be greater in the supercooled liquid than in the glass for standard conditions, numerical simulation show that the decrease in activation energy is the consequence of probing a very fragile system with heating rates high enough to probe the high temperature region of the fragile liquid where the activation energy becomes lower than that of the glass 14. This provides additional evidence that these PCMs indeed crystallize below $T_{\rm g}$.

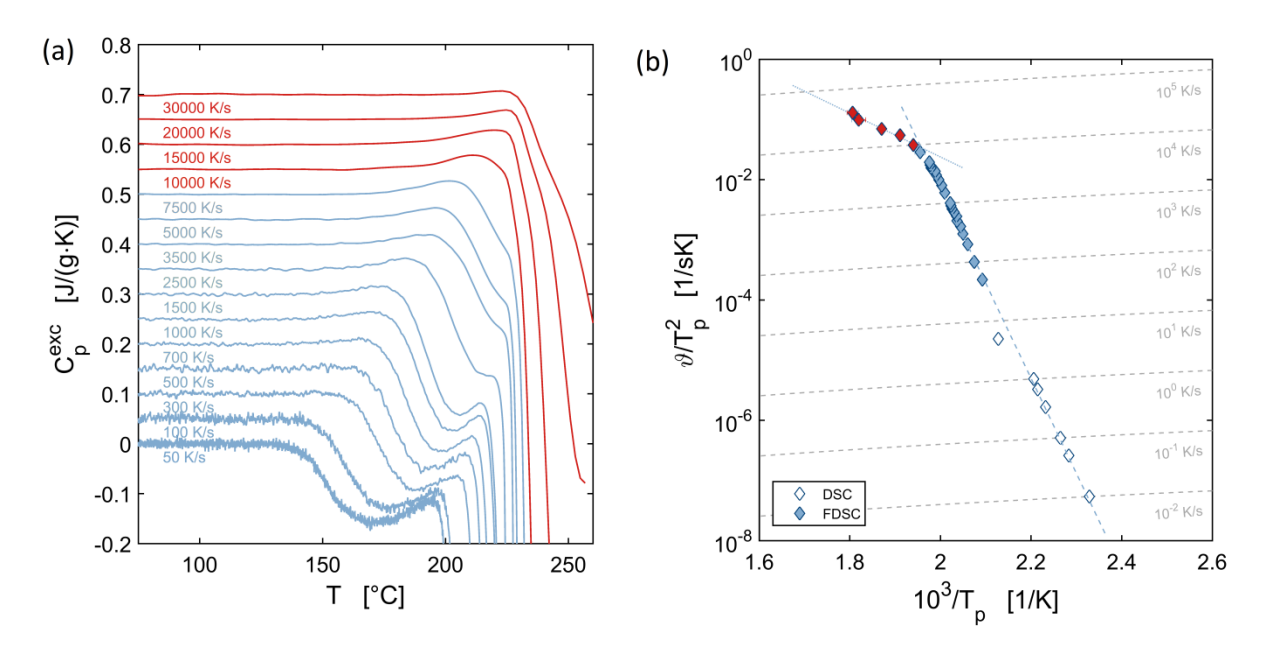


Figure 3: (a) Excess heat capacity thermograms of as-deposited Ge₂Sb₂Te₅ obtained by Flash-DSC at rate spanning 50 K/s to 30,000 K/s. (b) Kissinger plot for as-deposited Ge₂Sb₂Te₅ showing a sudden change in crystallization activation energy from 3.13 eV at low rates to 0.69 eV at high rates. (Data from Ref. [14])

It has been previously suggested that fast crystallization of PCMs cannot occur below the standard $T_{\rm g}$ due to the kinetic arrest characteristic of this temperature range²⁴. Below we use the

simple kinetic model developed by Turnbull³⁶ to show that hyperquenching and high fragility of PCMs drastically affect the crystallization kinetics and suggest that fast crystallization can occur below $T_{\rm g}$ directly from the glassy state.

Kinetic model for crystallization in hyperquenched systems:

Turnbull parameter:

In his seminal paper on glass formation³⁶ Turnbull derived the reduced glass temperature $T_{\rm rg} = T_{\rm g}/T_{\rm m}$ as a predictive metric for the ability of a system to bypass crystallization and form glass upon cooling. It was found that systems exhibiting $T_{\rm rg} > 2/3$ have exceedingly low nucleation rate I and can easily form a glass. For example, $T_{\rm rg} = 0.75$ for SiO₂ where nucleation is never observed experimentally upon cooling. Conversely, phase change materials are notoriously bad glass-formers and exhibit lower Turnbull parameters, i.e. $T_{\rm rg} = 0.46$ for GeTe. These predictions are based on the estimation of the temperature dependence of the nucleation rate as shown in Figure 4. These estimates result from the balance between the work required to overcome surface tension and the gain in free energy resulting from the growth of the nuclei. Nuclei reaching a critical radius $r_{\rm i}$ achieve that balance and can grow further due to an overall decrease in free energy. The growth of these critical nuclei proceeds from the addition of atoms through a diffusion mechanism. The process of transport across the nucleus-matrix interface is controlled by a free energy of activation ΔG and described by a diffusion coefficient D according to:

$$D = D_0 \exp\left(\frac{-\Delta G'}{kT}\right) \tag{1}$$

where D_0 is a constant, T the temperature and k is Boltzmann's constant. This constitutes the kinetic barrier to nucleation. The diffusion coefficient is then related to the viscosity η using the Stokes-Einstein equation:

$$D = \frac{kT}{3\pi a_0 \eta} \tag{2}$$

where a_o is the diameter of the diffusing species and η is the viscosity. Following the classical nucleation theory³⁷ (CNT), the nucleation rate can then be expressed as³⁶:

$$I = \frac{k_{\rm n}}{\eta} \exp\left[-\frac{16\pi\alpha^3\beta}{3T_{\rm r}(\Delta T_{\rm r})^2}\right]$$
 (3)

with the reduced temperature $T_{\rm r}=T/T_{\rm m}$, the reduced undercooling $\Delta T=(T_{\rm m}-T)/T_{\rm m}$ and where $k_{\rm n}$ is a constant, α is a dimensionless parameter related to the surface tension and β is a dimensionless parameter related to the entropy of melting. For small undercooling ($\Delta T_{\rm r}\sim 0$), the exponent term dominates and I vanishes, while for large undercooling the pre-exponent dominates due to the increase in equilibrium viscosity η (following the Vogel-Fulcher-Tammann (VFT) equation), and I vanishes again. At intermediate temperatures, I reaches large values that depends on the reduced glass temperature (Figure 4) as the equilibrium viscosity η is lower, the lower the reduced glass transition temperature $T_{\rm rg}$.

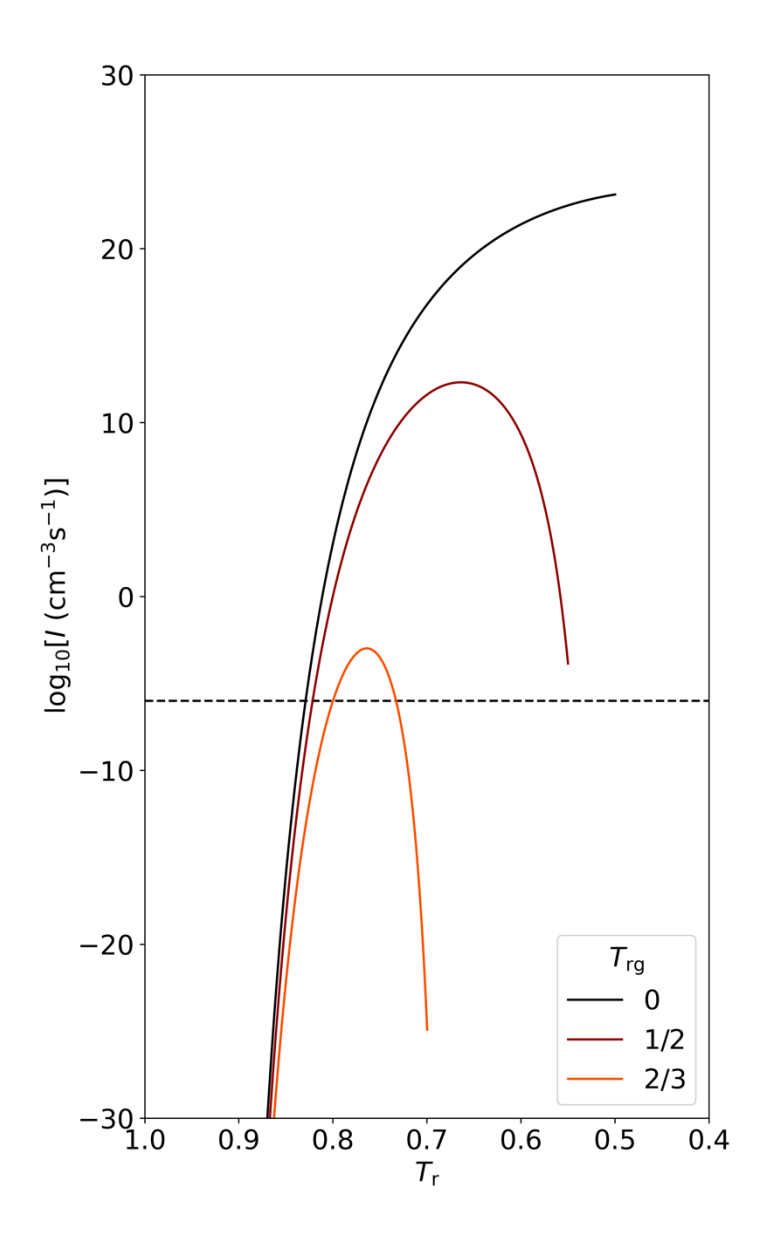


Figure 4: Estimation of the temperature dependence of the nucleation rates I using the Turnbull method for systems with different reduce glass temperature $T_{\rm rg}$. Reproduced from ref. [36]

The Turnbull model was developed based on the assumption that crystallites form in the undercooled liquid, however recent observations on poor glass-forming systems shown in the previous section suggest that crystallization may also take place rapidly from the glassy state. In this case the characteristic relaxation time that controls viscosity and diffusion should be determined by the isostructural viscosity rather than the equilibrium viscosity. This in turn should notably affect estimations of the nucleation rates at large undercooling. Moreover, these relaxation times are a function of temperature, time, as well as quenching rate (i.e. fictive temperature $T_{\rm f}$) and should affect crystallization kinetics accordingly as described in the next section.

Relaxation times:

The viscosity η is related to the stress relaxation time τ_S according to the Maxwell equation:

$$\eta = G_{\infty} \tau_{\rm S} \tag{4}$$

where G_{∞} is the instantaneous shear modulus and $\tau_{\rm S}$ represents the time constant for the system to respond to a mechanical stress at a given temperature (i.e beam bending, indentation, parallel plate, rotating cup, capillary etc.). Measurements performed in the stable liquid above $T_{\rm m}$ or the metastable undercooled liquid below $T_{\rm m}$ yield the equilibrium stress relaxation time $\tau_{\rm S(equ)}$ which increases exponentially with decreasing temperature as depicted schematically in Figure 5. Upon cooling at a standard rate of ~20 °C/min the system may vitrify at the glass transition temperature $T_{\rm g}$ when $\tau_{\rm S(equ)}$ reaches ~100 seconds (Figure 5). At any temperature below $T_{\rm g}$ the system is trapped in the glassy state and η is now controlled by the isostructural stress relaxation time $\tau_{S(iso)}$ which notably diverges from $\tau_{S(equ)}$ (Figure 5). It is noteworthy to point out that $\tau_{S(iso)}$ is several orders of magnitude shorter than $\tau_{S(equ)}$ at temperatures below T_g . In other words, the viscosity of a glass is several orders of magnitude lower than that of the corresponding equilibrium liquid at the same temperature. Importantly, this difference is further exacerbated in hyperquenched glasses where $\tau_{S(iso)}$ departs from $\tau_{S(equ)}$ at a higher temperature T_f . As shown by Moynihan et al. 38 , the greater the cooling rate, the greater the fictive temperature $T_{\rm f}$. Per equation (4) it results that the isostructural viscosity controlling crystallization below $T_{\rm g}$ is many orders of magnitude lower than the equilibrium viscosity originally used to estimate I in equation (3). To account for this divergence in viscosity at $T_{\rm g}$ we therefore use the Adam-Gibbs equation modified by Hodge³⁹ in equation (3). The results are shown in Figure 6 for two glasses of fragility m = 40 and m = 100 quenched at a rate of 10,000 K/s. Details of the calculation can be found in Supplementary Information. Figure 6 shows that the nucleation rate I of the hyperquenched glassy state can be many orders of magnitude faster than that of the equilibrium liquid at and below $T_{\rm g}$. This explains why some hyperquenched PCMs with poor glass-forming ability such as GeTe ($T_{rg} = 0.46$) can undergo fast crystallization even below the glass transition temperature. Other PCMs with better glass-forming ability such as $Ge_3Sb_6Te_5$ ($T_{rg} = 0.56$) from Figure 1 can exhibit a glass transition before crystallization i.e. the nucleation curve would be shifted down to low values of I (see Figure 4). The difference in crystallization behavior between these two systems can also be revealed through experimental measurement of their viscositytemperature dependence as shown in the following section.

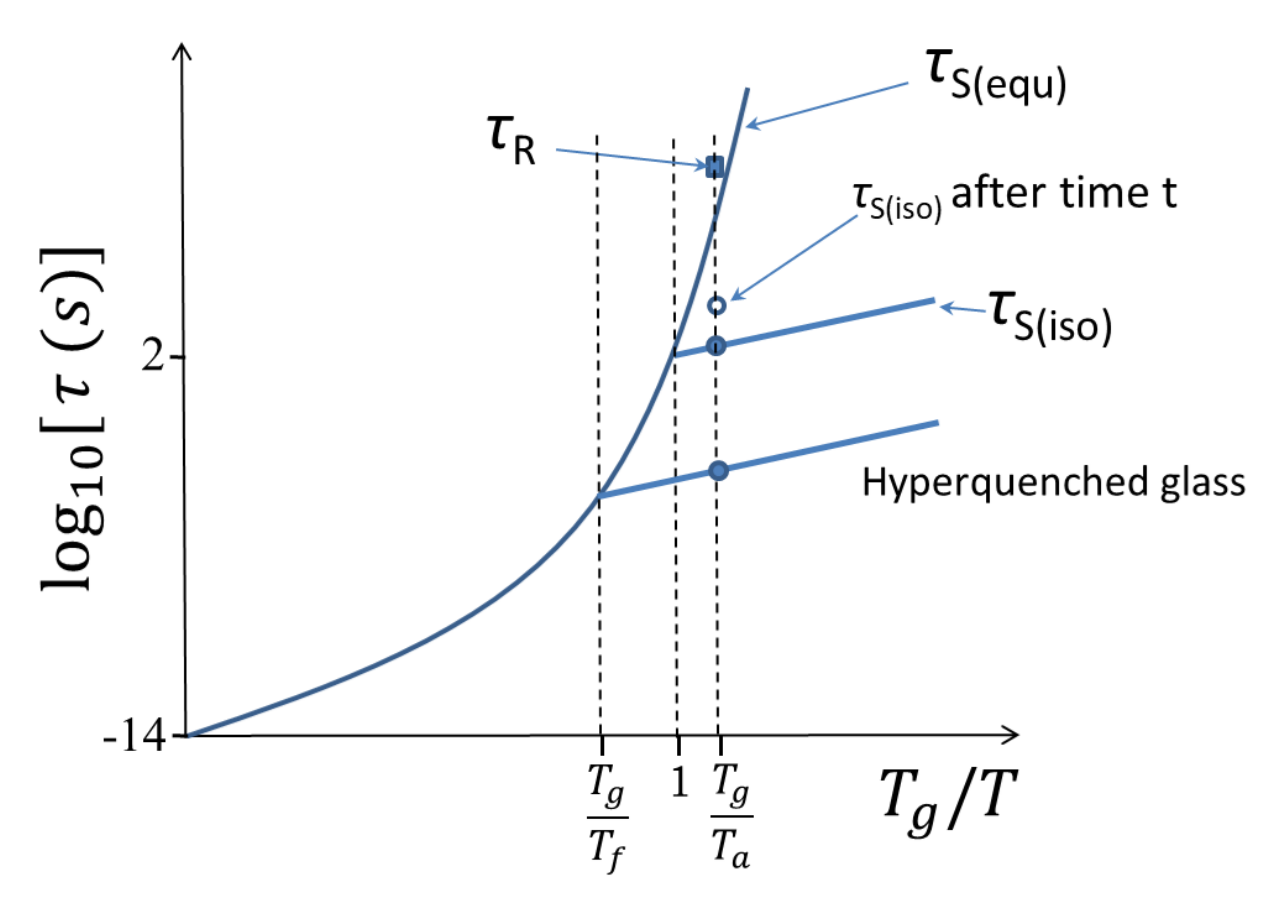


Figure 5: Schematics of the temperature dependence of the relaxation time in a glass-forming liquid. The solid line corresponds to the equilibrium stress relaxation $\tau_{S(equ)}$ while the dashed lines correspond to the isostructural stress relaxation time $\tau_{S(iso)}$ of the standard and hyperquenched glass. τ_R is the structural relaxation time (enthalpy, volume, refractive index etc.) measure without any applied stress. It represents the time that is needed for a glass to reach the equilibrium line. T_f is the fictive temperature of the hyperquenched glass and T_a is the annealing temperature.

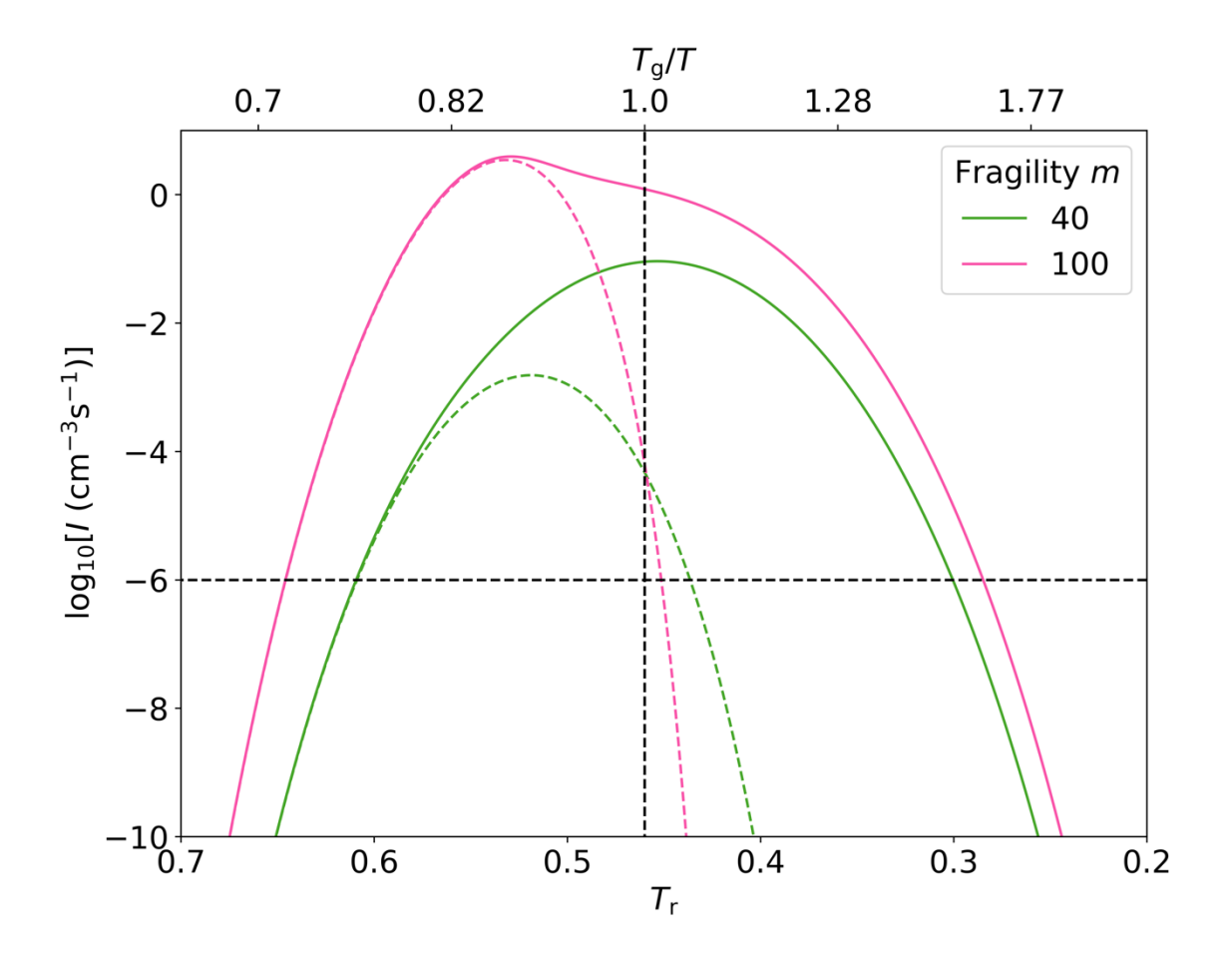


Figure 6: Nucleation rate I computed using the Turnbull method modified with the Adam-Gibbs equation to account for the change of viscosity at and below $T_{\rm g}$. Dotted lines are obtained using the equilibrium viscosity while solid line are obtained using the non-equilibrium isostructural viscosity in equation (3). Curves are shown for two glasses of fragility index m=40 and m=100 cooled at 10,000 K/s and with reduced glass temperature $T_{\rm rg} = 0.46$ corresponding to GeTe.

Fragile to strong transition:

The viscosity-temperature dependence of several PCMs is shown in Figure 7 over nearly 16 orders of magnitudes. Viscosity measurements over such broad range require multiple techniques including oscillating-cup viscometry, crystal growth velocity measurements from time-resolved reflectivity and transmission electron microscopy (TEM), as well as calorimetry. Experimental details about each method and the measurements on GeTe can be found in Ref. [20] and method section, respectively. Several features are noteworthy in the viscosity-temperature dependence presented in Figure 7. The first feature is a sudden change in fragility in the region $T_g/T = 0.6-0.7$. The liquids are initially strong at lower temperature with a fragility index near m = 40 and suddenly switch to a fragile behavior with a fragility index near m = 100. The full curve cannot be fitted with conventional models such as VFT or MYEGA⁴⁰ and therefore indicates a transition in fragility. This fragile to strong transition (FST) appears to be a common feature of PCMs^{20,41}.

Figure 6 compares the nucleation behavior of two systems with fragility index m = 40 and m = 100 analogous to those found on each side of the FST in the previous PCMs. Based on these results the FST is of significant benefit for PCM technology as it provides lower nucleation rate below $T_{\rm g}$ for increased stability of the memory cell and better data retention, while simultaneously providing higher nucleation rate at higher temperature for faster switching speed and rapid computing.

The second feature of interest in Figure 7 is the mismatch in viscosity between GeTe and $Ge_3Sb_6Te_5$ on approaching T_g . This pattern is reminiscent of the departure of $\tau_{S(iso)}$ from $\tau_{S(equ)}$ in Figure 5. Indeed Ge₃Sb₆Te₅ is a relatively good glass-former and all viscosity measurements are performed in the equilibrium supercooled liquid state down to $T_{\rm g}$ and slightly below²⁰. The system then exhibits the expected viscosity $\eta = 10^{12} \text{ Pa} \cdot \text{s}$ at T_g . No viscosity measurements were then performed in the glassy state for Ge₃Sb₆Te₅. In contrast, measurements performed on GeTe, at and below $T_{\rm g}$, show much lower viscosity than expected from equilibrium. This departure from equilibrium is consistent with measurements of isostructural viscosity in the glassy state 42,43. While these measurements unambiguously show that the system is trapped in a nonequilibrium state, the absolute value of viscosity should be subject to significant caveat. This is because the measurements take a certain amount of time during which the system may undergo structural relaxation as depicted in Figure 5 for an annealing temperature T_a near T_g . Hence, the measured viscosity may reflect an average value of an intermediate state between the original glass and a partially relaxed glass. Consequently, the viscosity data measured in the glassy phase does not reflect the isostructural viscosity of the glassy phase and thus a physically meaningful activation energy cannot be obtained. The effect of structural relaxation on the crystallization kinetics from the glassy state will be discussed in the following section.

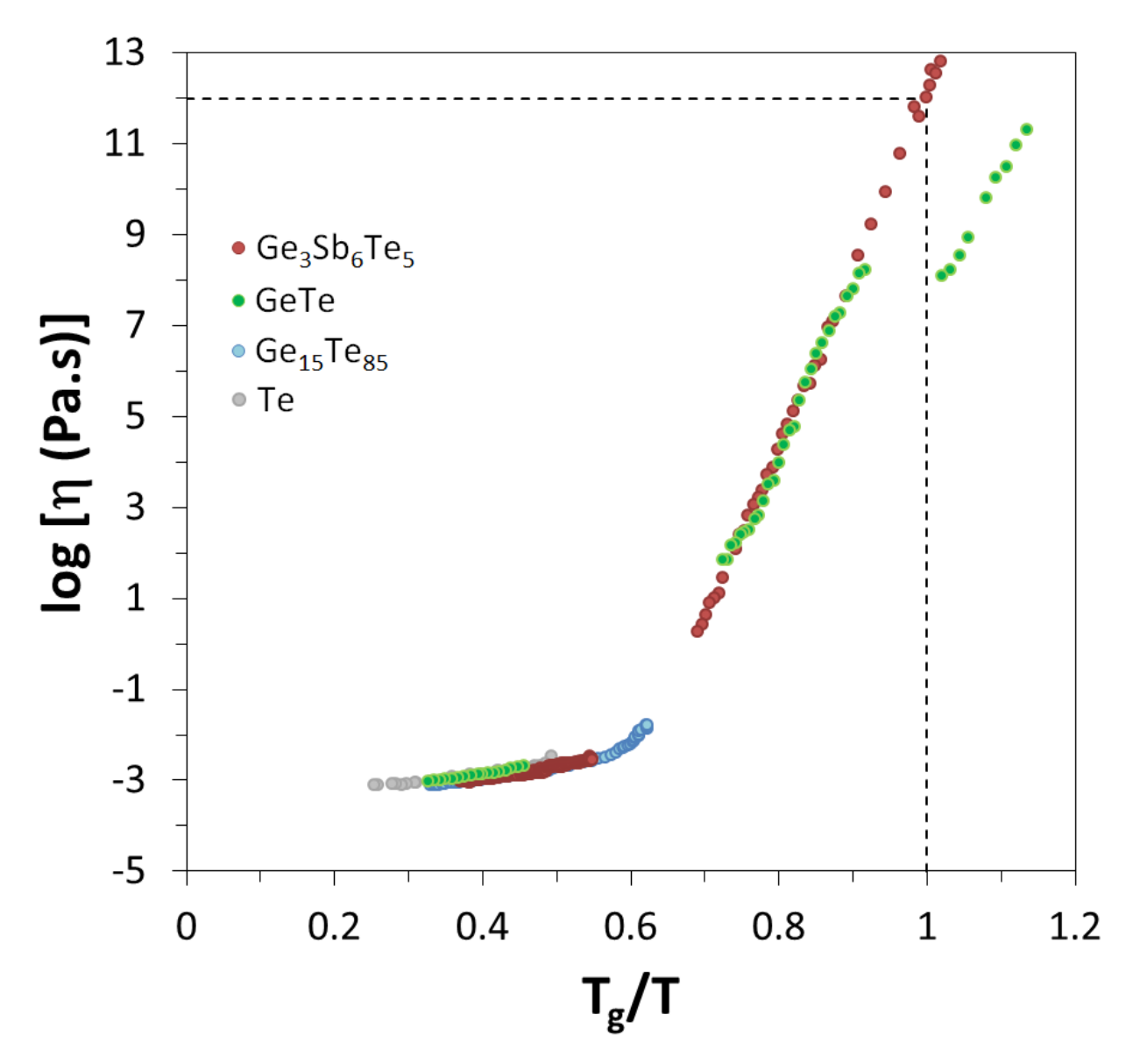


Figure 7: Viscosity-temperature dependence of $Ge_3Sb_6Te_5$, GeTe, $Ge_{15}Te_{85}^{44}$ and Te^{45} . Viscosity in the range 10^{-4} – 10^{-1} Pa·s was measured by oscillating-cup viscometry, in the range 1– 10^{8} Pa·s by time-resolved reflectivity and in the range 10^{8} – 10^{13} by in-situ transmission electron microscopy. Data for $Ge_3Sb_6Te_5$ are from Ref. [20] where a decoupling factor $\xi = 0.91$ between viscosity and diffusivity was found below T_g . Data for GeTe were collected for this work using the same method as for $Ge_3Sb_6Te_5$. The same decoupling factor $\xi = 0.91$ was used for GeTe. The time-resolved reflectivity data for GeTe exhibit greater noise due to occasional nucleation during the measurement that may affect the crystal growth velocity estimate.

Effect of structural relaxation on sub- T_g crystallization:

Figure 5 illustrate how $\tau_{S(iso)}$, given enough time, evolves towards $\tau_{S(equ)}$ due to the natural tendency of a glass to relax towards its equilibrium supercooled liquid state. The time constant τ_R necessary for this process has been shown to be slightly longer than $\tau_{S(equ)}$ and much longer than

 $\tau_{S(iso)}$ (Figure 5)^{42,46}. The crystallization kinetics controlled by $\tau_{S(iso)}$ in the glassy state should therefore slowly evolve in a way consistent with the dynamics of structural glass relaxation controlled by τ_R . Figure 8 shows how the maximum crystallization temperature T_P of a $Ge_2Sb_2Te_5$ glass ($T_g = 200$ °C) evolves over three years of annealing at 75 °C. The shift in T_P follows a non-exponential decay function of the Kohlrausch-Williams-Watts (KWW) 47,48 form that is characteristic of glass relaxation⁴⁹. The inset of Figure 8 shows that the enthalpy of fusion is constant and that the system has not significantly crystallized during annealing. The increase in $T_{\rm P}$ indicates that crystallization is being delayed as a result of annealing and requires higher thermal energy. This increase in crystallization temperature is opposite to that expected if the system had nucleated during the annealing procedure. Yet, fluctuation electron microscopy (FEM) and TEM analysis of Ge₂Sb₂Te₅ before and after annealing reveal an increase in number of sub-critical nuclei (Figure 9)¹⁴. The FEM variance that is a measure of medium range order and oftentimes interpreted as an increase in the sub-critical nuclei distribution increases during annealing as shown in Figure 9(a). After annealing some nanodiffraction patterns taken for FEM reveal nanocrystalline diffraction spot which were not found in the as-deposited (un-annealed) state as shown in Figure 9(c&d), indicating an increase in critical nuclei number. Finally the number of grains obtained by TEM imaging following annealing at 115 °C and crystallization at 150 °C show a significant increase because of the pre-annealing treatment as shown in Figure 9(b)¹⁴. The presence of these subcritical nuclei should favor crystallization and lower the crystallization temperature, contrary to the shift observed experimentally in Figure 8. Another more significant contribution must therefore hinder crystallization during annealing. This contribution is the increase in isotructural viscosity $\eta_{(iso)}$ expected from the relaxation process depicted in Figure 5 and observed experimentally in amorphous chalcogenides⁴³. An increase in viscosity is expected to lower both crystal growth and nucleation rate (equation 3) and should therefore delay crystallization to higher temperature during heating at constant rate, as observed experimentally. This also means that the effect of increased viscosity due to glass aging outperforms the increase in nucleation tendency deduced from the rise in FEM variance during pre-annealing.

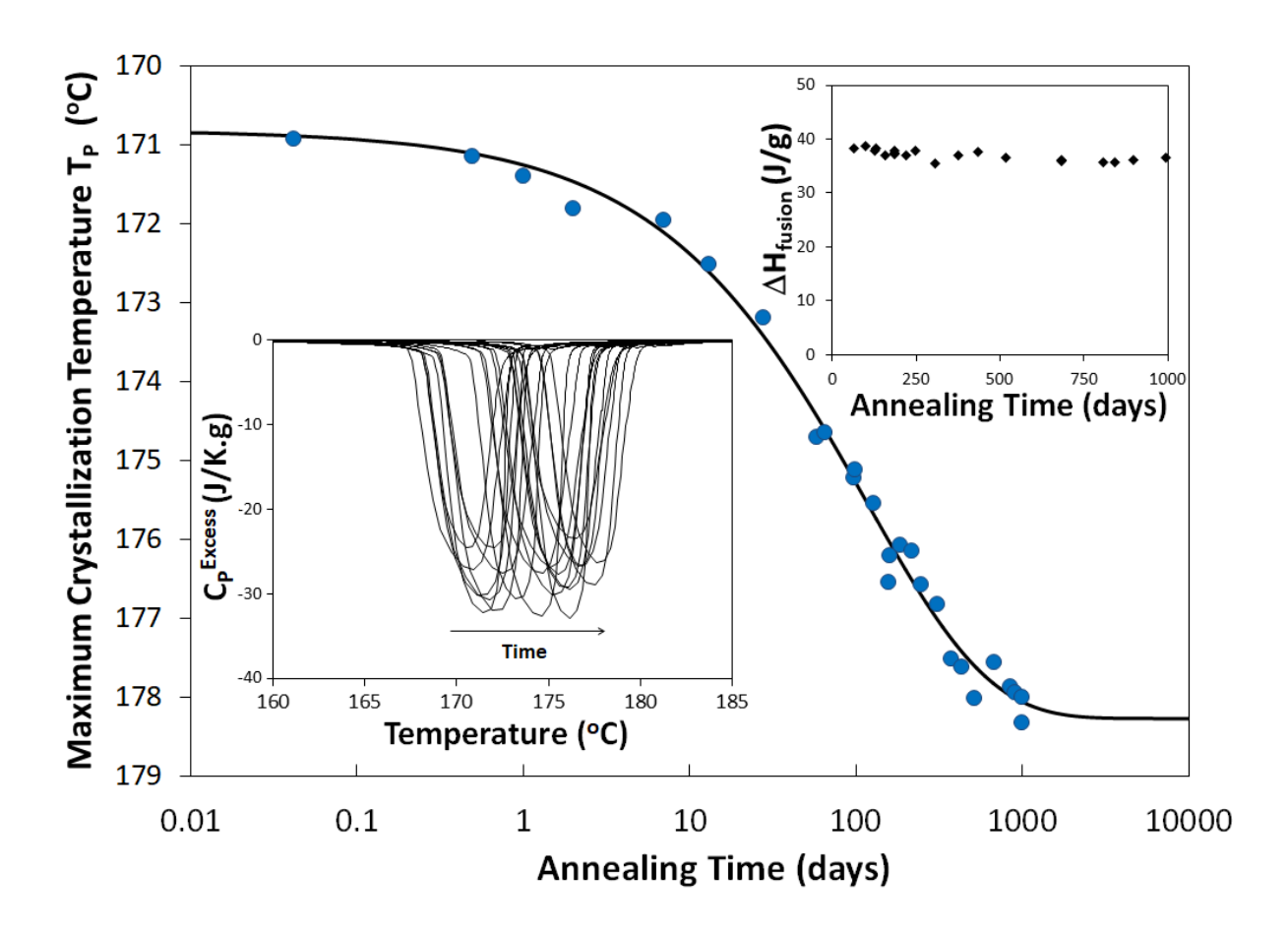


Figure 8: Evolution of the maximum crystallization temperature T_P of a $Ge_2Sb_2Te_5$ glass during annealing at 75 °C. The lower left inset shows the upward shift of the crystallization exotherm as a function of annealing time. The upper right inset shows that the enthalpy of fusion remains mainly constant throughout the annealing procedure.

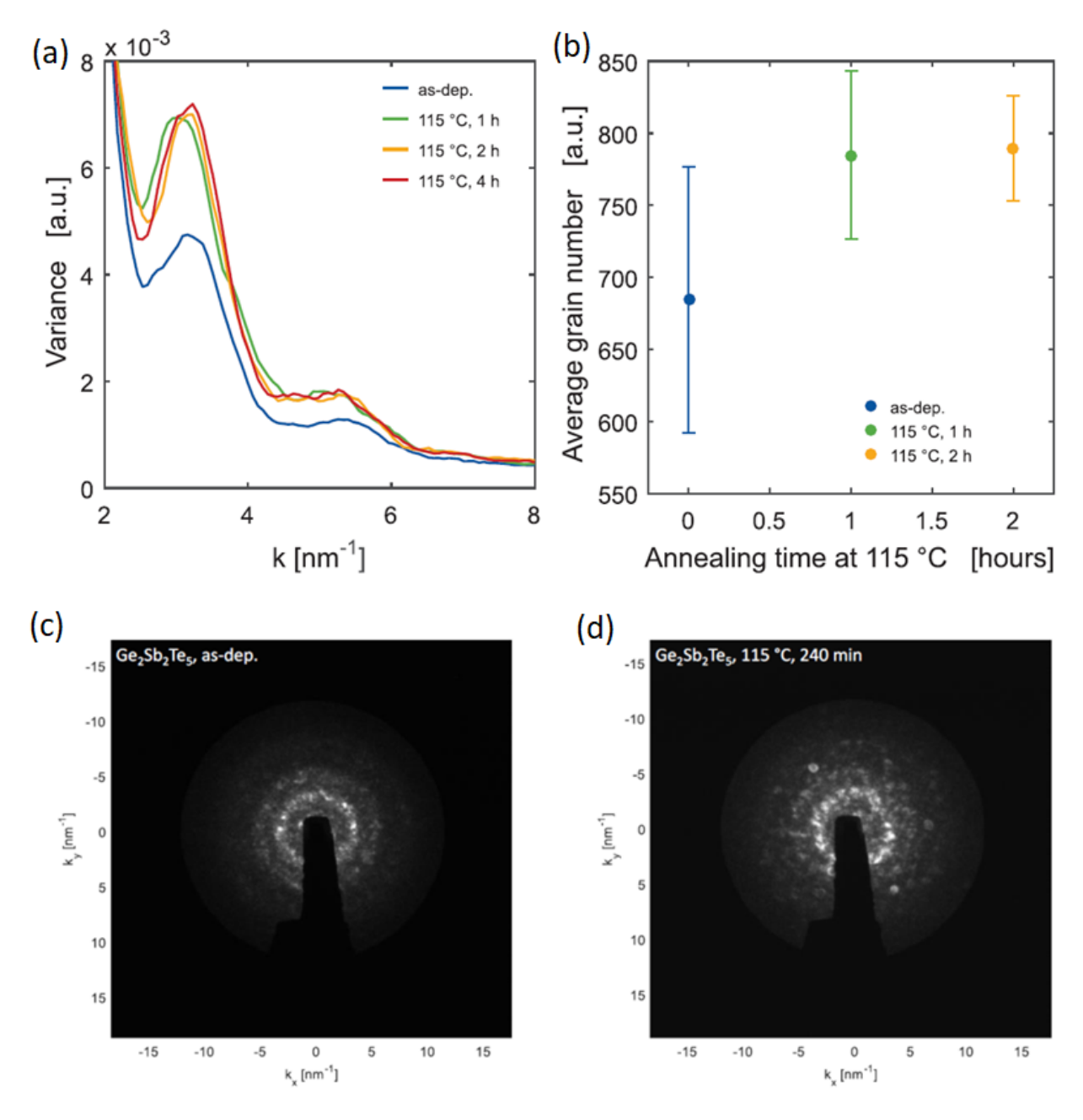


Figure 9: (a) Fluctuation electron microscopy variance of a Ge₂Sb₂Te₅ glass after annealing at 115 °C. An increase in variance indicates an increase in medium range order. (b) Average grain number obtained from TEM image analysis after annealing Ge₂Sb₂Te₅ glass at 115 °C following crystallization at 150 °C for one hour. (c) Nanodiffraction pattern collected before annealing and (d) after annealing at 115 °C showing an increase in nanocrystalline diffraction spots. Note, that diffraction patterns showing nanocrystalline diffraction patterns are excluded from the FEM calculation in (a) in order to investigate the medium range order change in the purely amorphous phase. Figures adapted from Ref. [14].

The non-exponential decay of T_P observed in Figure 8 is characteristic of glass structure relaxation dynamics⁵⁰. Dynamic heterogeneities intrinsic to glasses result in a distribution of relaxation times and a non-exponential relaxation process⁵¹. The fit shown in Figure 8 yields a non-exponential factor $\beta = 0.59$ and a characteristic relaxation time $\tau = 116$ days (10⁷ s). This magnitude of relaxation time is consistent with that of structural relaxation in glass far below T_g . Overall the results of Figure 8 further support the conclusion that PCMs can crystallize from the glassy state when reheated at standard rates.

Discussion

Crystallization below the glass transition temperature $T_{\rm g}$ is not uncommon. In particular, organic glasses frequently exhibit unusually high crystallization rates below $T_{\rm g}^{2-9}$. These unexpectedly fast crystallizations are the result of a decoupling between diffusivity and viscous flow which is exacerbated by high fragility⁵². Nevertheless, these system are fairly good glass-formers that exhibit a clear glass transition when measured at the standard rate of 20 °C/min. On the other end, very poor glass formers that require hyperquenching to vitrify such as PCMs, do not exhibit a calorimetric glass transition when reheated at standard rates. While they also undergo a decoupling between diffusivity and viscous flow on approaching $T_{\rm g}$, they are also subjected to very high fictive temperatures that considerably lowers their isostructural viscosity. These low effective viscosity promotes both fast nucleation and fast crystal growth. As a consequence, they systematically crystallize prior to reaching $T_{\rm g}$ when reheated at standard rates.

The Turnbull parameter $T_{\rm rg}$ is generally reliable and has been broadly used in the glass community to assess glass-forming ability⁵³. Consistent trends in Turnbull parameter can be observed in PCMs where compounds with low parameter values such as GeTe ($T_{\rm rg} = 0.46$) and ${\rm Ge_2Sb_2Te_5}$ ($T_{\rm rg} = 0.52$) are very poor glass former without measurable calorimetric $T_{\rm g}$, while compounds with higher parameter values such as ${\rm Ge_3Sb_6Te_5}$ ($T_{\rm rg} = 0.56$) and ${\rm GeSe}$ ($T_{\rm rg} = 0.58$) are better glass-former with a distinct glass transition endotherm. Nevertheless, some notable exception exist such as AIST ($T_{\rm rg} = 0.56$) which does not exhibit a glass transition at standard heating rate despite its high Turnbull parameter¹⁵. This indicates that other contributions besides the thermodynamic factors governing the difference between $T_{\rm g}$ and $T_{\rm m}$ must play a significant role in controlling crystallization kinetics. In particular, it was recently shown that glass-formation and crystallization rates were strongly dependent on bonding characteristics in PCMs¹⁹.

Crystalline phase change materials such as GeTe, $Ge_2Sb_2Te_5$ and Sb_2Te_3 are characterized by an unconventional bonding mechanism, which differs from ionic, metallic and covalent bonding ⁵⁴. The bonding has been denoted as metavalent bonding (MVB). This bonding mechanism is characterized by an unconventional property portfolio including a large chemical bond polarizability as evidenced by high values of the Born effective charge Z^* and high values of ε_∞ , the optical dielectric constant ^{55,56}. MVB is also characterized by an unconventional bond rupture upon laser-assisted field evaporation ⁵⁷. Characteristic for this bonding mechanism is a competition between electron delocalization as in metallic bonding and electron localization as in covalent or ionic bonding. As a consequence, interfacial energies between the undercooled liquid and the crystalline phase are quite low, despite the pronounced change in atomic arrangement ⁵⁸.

MVB solids have a small electron transfer between atoms and share only about half an electron pair between adjacent atoms, unlike covalent solids, where about one electron pair is formed, e.g. for Diamond⁵⁹. In a map, metavalent solids are hence located between metals and covalently bonded solids. Compounds like GeTe, but also Sb₂Te₃⁶⁰ and PbSe⁶¹, employ this bonding mechanism. The distinct nature of this bond is also supported by pronounced property changes upon the transition from metavalent to covalent bonding.

In the amorphous phase, where the bonding is supposed to be covalent, locally ordered regions averaging one shared electron per bond (about half an electron pair) such as four-fold rings are also believed to play a role in the fast crystallization kinetics of some systems 62,63 . Furthermore, the small interfacial energy at elevated temperatures helps to realize a high crystallization speed 58 . Meanwhile, the more pronounced Peierls distortion near and below $T_{\rm g}$ stabilizes the glassy phase 64 . Hence, multiple factors are at play in predicting crystallization speed and glassforming ability. More systematic studies of thermodynamic, kinetic and chemical bonding properties may reveal whether or not they are related to a common physical origin.

Conclusion:

Very poor glass-formers can only be vitrified through hyperquenching. They can be found across a broad category of materials including PCMs, some metallic alloys and molecular liquids such as water. Interestingly, they share a common calorimetric feature in that they do not exhibit a glass transition endotherm prior to crystallization. Using the case of PCMs this study has shown that these amorphous solids can crystallize below the glass transition. Evidence for this process includes the appearance of a glass transition endotherm at ultra-fast heating rates concomitant with a sudden change in crystallization kinetics as the system switches from crystallizing from the glassy to the liquid state. Additionally, the pre- $T_{\rm g}$ relaxation exotherm can only be rationalized if the $T_{\rm g}$ lays above the crystallization exotherm during a standard heating ramp. Moreover, the maximum crystallization temperature T_p is found to increase with annealing time despite the more abundant sub-critical nuclei that should speed up crystallization. This observation is not consistent with crystallization from the liquid state but is consistent with an increase in isostructural viscosity during structural relaxation of the glass. This is confirmed by the non-exponential decay of the shift in T_p that is characteristic of the dynamic heterogeneity intrinsic to glasses. The characteristic time of 116 days associated with this process is also consistent with sub- $T_{\rm g}$ structural relaxation. Finally, modeling based on the Turnbull equation shows that nucleation kinetics are indeed high even below $T_{\rm g}$ due to the hyperquenched nature of the system. This supports the ability of the system to undergo crystallization prior to the glass transition upon slow heating. The model also shows that the fragile-to-strong transition observed in PCMs is advantageous to slow down crystallization at low temperature while increasing its speed at higher temperature.

Experimental section:

<u>Viscosity measurement</u>: The viscosity of GeTe presented in Figure 7 is determined from two types of crystal growth velocity measurements. On the one hand, samples prepared by magnetron sputter deposition were annealed isothermally in a differential scanning calorimeter (DSC) and

the nucleated grains and their growth was investigated by transmission electron microscopy (TEM) for at least three times. Using the TEM method, the crystal growth velocity of the asdeposited phase is measured at temperatures from 135 °C up to 180 °C. For the highest treatment temperatures, the samples were dipped in an pre-heated oil bath and rapidly quenched in a room temperature bath of ethylene glycol, which allowed for annealing times on the timescale of seconds. The initially amorphous GeTe layer is 30 nm thick and encapsulated between two inert capping layers of (ZnS)₈₀:(SiO₂)₂₀ which is supported by a Si₃N₄ layer.

On the other hand, the crystal growth velocity is measured in a laser reflectivity setup. Here the samples from the same magnetron deposition run were used in order to ensure highest comparability between the measurement techniques. The samples were crystallized and brought the temperature where the crystal growth velocity is supposed to be measured. Then a laser pulse is used to melt-quench a 1.5 µm diameter spot to the amorphous phase which induces a reflectivity change. Upon recrystallization of the melt-quenched amorphous spot, the reflectivity increases back to its original value. From this time resolved reflectivity measurements, the crystal growth velocity is determined in the temperature range from 231.5 °C up to 365 °C. More information on both methods are reported in Ref. [20].

<u>Calorimetry</u>: Enthalpy recovery exotherm for Ge₂Sb₂Te₅ and AIST in Figure 2 and maximum crystallization temperature T_P of Ge₂Sb₂Te₅ in Figure 8 were collected using a TA Q1000 DSC. A glass sample mass of 8-10 mg was sealed in an aluminum pan and an empty pan was used as a reference. Temperature was calibrated with an indium standard and heat flow was calibrated with a sapphire standard. For the annealing procedure, 26 samples of Ge₂Sb₂Te₅ were sealed in an aluminum pan and introduced in an incubator at a temperature of 75 °C. Temperature stability was within 0.5 °C. At various time intervals, samples were removed from the incubator and allowed to cool down before being introduced in the DSC for measurement.

Supplementary Material

See supplementary material for details of the numerical simulation of the nucleation rate in the equilibrium and at the non-equilibrium state.

Acknowledgements:

PL acknowledges financial support from NSF-DMR under grant#: 1832817. Some of us (JP, MW) acknowledge funding in part from the Deutsche Forschungsgemeinschaft (DFG) via the collaborative research center Nanoswitches (SFB 917) and in part from the Federal Ministry of Education and Research (BMBF, Germany) in the project NEUROSYS (03ZU1106BA).

Data Availability:

The data that support the findings of this study are available from the corresponding author upon reasonable request.

References:

Fokin, V. M., Abyzov, A. S., Yuritsyn, N. S., Schmelzer, J. W. P. & Zanotto, E. D. Effect of structural relaxation on crystal nucleation in glasses. *Acta Materialia* **203**, 116472, (2021), doi:https://doi.org/10.1016/j.actamat.2020.11.014.

- Hikima, T., Adachi, Y., Hanaya, M. & Oguni, M. Determination of potentially homogeneousnucleation-based crystallization in o-terphenyl and an interpretation of the nucleationenhancement mechanism. *Physical Review B* **52**, 3900-3908, (1995), doi:10.1103/PhysRevB.52.3900.
- Ishida, H., Wu, T. & Yu, L. Sudden Rise of Crystal Growth Rate of Nifedipine near Tg without and with Polyvinylpyrrolidone. *Journal of Pharmaceutical Sciences* **96**, 1131-1138, (2007), doi:https://doi.org/10.1002/jps.20925.
- Schammé, B., Monnier, X., Couvrat, N., Delbreilh, L., Dupray, V., Dargent, É. & Coquerel, G. Insights on the Physical State Reached by an Active Pharmaceutical Ingredient upon High-Energy Milling. *The Journal of Physical Chemistry B* **121**, 5142-5150, (2017), doi:10.1021/acs.jpcb.7b02247.
- Willart, J.-F., Carpentier, L., Danède, F. & Descamps, M. Solid-State Vitrification of Crystalline Griseofulvin by Mechanical Milling. *Journal of Pharmaceutical Sciences* **101**, 1570-1577, (2012), doi:https://doi.org/10.1002/jps.23041.
- Wu, T. & Yu, L. Surface Crystallization of Indomethacin Below Tg. *Pharmaceutical Research* **23**, 2350-2355, (2006), doi:10.1007/s11095-006-9023-4.
- 7 Zhu, L., Wong, L. & Yu, L. Surface-Enhanced Crystallization of Amorphous Nifedipine. *Molecular Pharmaceutics* **5**, 921-926, (2008), doi:10.1021/mp8000638.
- Sun, Y., Xi, H., Chen, S., Ediger, M. D. & Yu, L. Crystallization near Glass Transition: Transition from Diffusion-Controlled to Diffusionless Crystal Growth Studied with Seven Polymorphs. *The Journal of Physical Chemistry B* **112**, 5594-5601, (2008), doi:10.1021/jp7120577.
- 9 Powell, C. T., Xi, H., Sun, Y., Gunn, E., Chen, Y., Ediger, M. D. & Yu, L. Fast Crystal Growth in o-Terphenyl Glasses: A Possible Role for Fracture and Surface Mobility. *The Journal of Physical Chemistry B* **119**, 10124-10130, (2015), doi:10.1021/acs.jpcb.5b05389.
- Yue, Y. & Angell, C. A. Clarifying the glass-transition behaviour of water by comparison with hyperquenched inorganic glasses. *Nature* **427**, 717-20, (2004).
- 11 Velikov, V., Borick, S. & Angell, C. A. The glass transition of water, based on hyperquenching experiments. *Science* **294**, 2335-8, (2001).
- Starink, M. J. Analysis of aluminium based alloys by calorimetry: quantitative analysis of reactions and reaction kinetics. *International Materials Reviews* **49**, 191-226, (2004), doi:10.1179/095066004225010532.
- Mendes, M. A. B., Kiminami, C. S., Botta Filho, W. J., Bolfarini, C., Falcao de Oliveira, M. & Kaufman, M. J. Crystallization behavior of amorphous Ti51.1Cu38.9Ni10 alloy. *Mater. Res. (Sao Carlos, Braz.)* **18**, 104-108, (2015), doi:10.1590/1516-1439.343014.
- Pries, J., Wei, S., Wuttig, M. & Lucas, P. Switching between Crystallization from the Glassy and the Undercooled Liquid Phase in Phase Change Material Ge2Sb2Te5. *Advanced Materials*, 1900784, (2019), doi:10.1002/adma.201900784.
- Pries, J., Sehringer, J. C., Wei, S., Lucas, P. & Wuttig, M. Glass transition of the phase change material AIST and its impact on crystallization. *Materials Science in Semiconductor Processing* **134**, 105990, (2021), doi:https://doi.org/10.1016/j.mssp.2021.105990.
- Pries, J., Yu, Y., Kerres, P., Häser, M., Steinberg, S., Gladisch, F., Wei, S., Lucas, P. & Wuttig, M. Approaching the Glass Transition Temperature of GeTe by Crystallizing Ge15Te85. *physica status solidi (RRL) Rapid Research Letters* **15**, 2000478, (2021), doi:https://doi.org/10.1002/pssr.202000478.
- Johari, G. P. Does water need a new Tg? *The Journal of Chemical Physics* **116**, 8067-8073, (2002), doi:10.1063/1.1466469.

- Lucas, P., Pries, J., Wei, S. & Wuttig, M. The glass transition of water, insight from phase change materials. *Journal of Non-Crystalline Solids: X* **14**, 100084, (2022), doi:https://doi.org/10.1016/j.nocx.2022.100084.
- Persch, C., Müller, M. J., Yadav, A., Pries, J., Honné, N., Kerres, P., Wei, S., Tanaka, H., Fantini, P., Varesi, E., Pellizzer, F. & Wuttig, M. The potential of chemical bonding to design crystallization and vitrification kinetics. *Nature Communications* 12, 4978, (2021), doi:10.1038/s41467-021-25258-3.
- Pries, J., Weber, H., Benke-Jacob, J., Kaban, I., Wei, S., Wuttig, M. & Lucas, P. Fragile-to-Strong Transition in Phase-Change Material Ge3Sb6Te5. *Advanced Functional Materials* **32**, 2202714, (2022), doi:https://doi.org/10.1002/adfm.202202714.
- Yue, Y. Revealing the nature of glass by the hyperquenching-annealing-calorimetry approach. *Journal of Non-Crystalline Solids: X* **14**, 100099, (2022), doi:https://doi.org/10.1016/j.nocx.2022.100099.
- Morales-Sánchez, E., Prokhorov, E. F., Mendoza-Galván, A. & González-Hernández, J. Determination of the glass transition and nucleation temperatures in Ge2Sb2Te5 sputtered films. *Journal of Applied Physics* **91**, 697-702, (2002), doi:10.1063/1.1427146.
- J.A. Kalb, M. Wuttig & Spaepen, F. Calorimetric measurements of structural relaxation and glass transition temperatures in sputtered films of amorphous Te alloys used for phase change recording. *J. Mat. Res* **22**, 748-754, (2007).
- Orava, J., Greer, A. L., Gholipour, B., Hewak, D. W. & Smith, C. E. Characterization of supercooled liquid Ge2Sb2Te5 and its crystallization by ultrafast-heating calorimetry. *Nat. Mater.* **11**, 279-283, (2012), doi:10.1038/nmat3275.
- 25 Cho, J.-Y., Kim, D., Park, Y.-J., Yang, T.-Y., Lee, Y.-Y. & Joo, Y.-C. The phase-change kinetics of amorphous Ge2Sb2Te5 and device characteristics investigated by thin-film mechanics. *Acta Mater.* **94**, 143-151, (2015), doi:10.1016/j.actamat.2015.04.058.
- Sebastian, A., Le Gallo, M. & Krebs, D. Crystal growth within a phase change memory cell. *Nature Communications* **5**, 4314, (2014), doi:10.1038/ncomms5314 https://www.nature.com/articles/ncomms5314#supplementary-information.
- Orava, J., Hewak, D. W. & Greer, A. L. Fragile-to-Strong Crossover in Supercooled Liquid Ag-In-Sb-Te Studied by Ultrafast Calorimetry. *Adv. Funct. Mater.* **25**, 4851-4858, (2015), doi:10.1002/adfm.201501607.
- Velikov, V., Borick, S. & Angell, C. A. Molecular Glasses with High Fictive Temperatures for Energy Landscape Evaluations. *The Journal of Physical Chemistry B* **106**, 1069-1080, (2002), doi:10.1021/jp012001z.
- 29 Chen, H. S. & Coleman, E. Structure relaxation spectrum of metallic glasses. *Applied Physics Letters* **28**, 245-247, (1976), doi:10.1063/1.88725.
- Hu, L., Zhang, C. & Yue, Y. Structural evolution during the sub-Tg relaxation of hyperquenched metallic glasses. *Appl. Phys. Lett.* **96**, 221908/1-221908/3, (2010), doi:10.1063/1.3447373.
- Yue, Y. Z., Jensen, S. L. & deC. Christiansen, J. Physical aging in a hyperquenched glass. *Applied Physics Letters* **81**, 2983-2985, (2002), doi:doi:http://dx.doi.org/10.1063/1.1514386.
- Huang, J. & Gupta, P. K. Enthalpy relaxation in thin glass fibers. *Journal of Non-Crystalline Solids* **151**, 175-181, (1992), doi:http://doi.org/10.1016/0022-3093(92)90026-G.
- Hu, L. & Yue, Y. Secondary Relaxation Behavior in a Strong Glass. *J. Phys. Chem. B* **112**, 9053-9057, (2008), doi:10.1021/jp711696p.
- Henderson, D. W. Thermal analysis of non-isothermal crystallization kinetics in glass forming liquids. *Journal of Non-Crystalline Solids* **30**, 301-315, (1979), doi:https://doi.org/10.1016/0022-3093(79)90169-8.

- Kissinger, H. E. Reaction Kinetics in Differential Thermal Analysis. *Analytical Chemistry* **29**, 1702-1706, (1957), doi:10.1021/ac60131a045.
- Turnbull, D. Under what conditions can a glass be formed? *Contemporary Physics* **10**, 473-488, (1969), doi:10.1080/00107516908204405.
- Volmer, M. & Weber, A. Nucleus formation in supersaturated systems. *Z. physik. Chem.* **119**, 277-301, (1926).
- Moynihan, C. T. & Macedo, P. B. Dependence of the glass transition temperature on heating rate and thermal history. *J. Phys. Chem.* **75**, 3379-81, (1971), doi:10.1021/j100690a033.
- Hodge, I. M. Adam-Gibbs formulation of nonlinearity in glassy-state relaxations. *Macromolecules* **19**, 936-8, (1986), doi:10.1021/ma00157a082.
- 40 Mauro, J. C., Yue, Y., Ellison, A. J., Gupta, P. K. & Allan, D. C. Viscosity of glass-forming liquids. *Proc. Natl. Acad. Sci. U. S. A.* **106**, 19780-19784, (2009), doi:10.1073/pnas.0911705106.
- Zalden, P., Quirin, F., Schumacher, M., Siegel, J., Wei, S., Koc, A., Nicoul, M., Trigo, M., Andreasson, P., Enquist, H., Shu, M. J., Pardini, T., Chollet, M., Zhu, D., Lemke, H., Ronneberger, I., Larsson, J., Lindenberg, A. M., Fischer, H. E., Hau-Riege, S., Reis, D. A., Mazzarello, R., Wuttig, M. & Sokolowski-Tinten, K. Femtosecond x-ray diffraction reveals a liquid–liquid phase transition in phase-change materials. *Science* 364, 1062, (2019), doi:10.1126/science.aaw1773.
- Lancelotti, R. F., Cassar, D. R., Nalin, M., Peitl, O. & Zanotto, E. D. Is the structural relaxation of glasses controlled by equilibrium shear viscosity? *Journal of the American Ceramic Society* **104**, 2066-2076, (2021), doi:https://doi.org/10.1111/jace.17622.
- C. Bernard, G. Delaizir, J.-C. Sangleboeuf, V. Keryvin, P. Lucas, B. Bureau, X. H. Zhang & Rouxel, T. Room temperature viscosity and delayed elasticity in infrared glass fiber. *J. Euro. Cer. Soc.* **27**, 3253, (2007).
- Weber, H., Orava, J., Kaban, I., Pries, J. & Greer, A. L. Correlating ultrafast calorimetry, viscosity, and structural measurements in liquid GeTe and Ge₁₅Te₈₅. *Physical Review Materials* **2**, 093405, (2018), doi:10.1103/PhysRevMaterials.2.093405.
- 45 Glazov, V. M. & Shchelikov, O. D. Change in short-range order structure in selenium and tellurium melts during heating. *Izv. Akad. Nauk SSSR, Neorg. Mater.* **10**, 202-7, (1974).
- Doss, K., Wilkinson, C. J., Yang, Y., Lee, K.-H., Huang, L. & Mauro, J. C. Maxwell relaxation time for nonexponential α-relaxation phenomena in glassy systems. *Journal of the American Ceramic Society* **103**, 3590-3599, (2020), doi:https://doi.org/10.1111/jace.17051.
- Kohlrausch, R. Theorie des elektrischen Rückstandes in der Leidener Flasche. *Annalen der Physik und Chemie* **167**, 56-82, (1854), doi:10.1002/andp.18541670103.
- Williams, G. & Watts, D. C. Non-symmetrical dielectric relaxation behaviour arising from a simple empirical decay function. *Transactions of the Faraday Society* **66**, 80-85, (1970), doi:10.1039/tf9706600080.
- 49 Moynihan, C. T. Structural relaxation and the glass transition. *Rev. Mineral.* **32**, 1-19, (1995).
- Boehmer, R., Ngai, K. L., Angell, C. A. & Plazek, D. J. Nonexponential relaxations in strong and fragile glass formers. *J. Chem. Phys.* **99**, 4201-9, (1993), doi:10.1063/1.466117.
- Ediger, M. D., Angell, C. A. & Nagel, S. R. Supercooled Liquids and Glasses. *J. Phys. Chem.* **100**, 13200-13212, (1996), doi:10.1021/jp953538d.
- Ediger, M. D., Harrowell, P. & Yu, L. Crystal growth kinetics exhibit a fragility-dependent decoupling from viscosity. *J. Chem. Phys.* **128**, 034709/1-034709/6, (2008), doi:10.1063/1.2815325.
- Nascimento, M. L. F., Souza, L. A., Ferreira, E. B. & Zanotto, E. D. Can glass stability parameters infer glass forming ability? *Journal of Non-Crystalline Solids* **351**, 3296-3308, (2005), doi:https://doi.org/10.1016/j.jnoncrysol.2005.08.013.

- Kooi, B. J. & Wuttig, M. Chalcogenides by Design: Functionality through Metavalent Bonding and Confinement. *Advanced Materials* **32**, 1908302, (2020), doi:https://doi.org/10.1002/adma.201908302.
- Wuttig, M., Deringer, V. L., Gonze, X., Bichara, C. & Raty, J.-Y. Incipient Metals: Functional Materials with a Unique Bonding Mechanism. *Advanced Materials* **30**, 1803777, (2018), doi:https://doi.org/10.1002/adma.201803777.
- C.-F. Schön, S. van Bergerem, C. Mattes, A. Yadav, M. Grohe, L. Kobbelt & Wuttig, M. Classification of properties and their relation to chemical bonding: Essential steps towards the inverse design of materials with tailored functionalities. *Science Advances* in press.
- Zhu, M., Cojocaru-Mirédin, O., Mio, A. M., Keutgen, J., Küpers, M., Yu, Y., Cho, J.-Y., Dronskowski, R. & Wuttig, M. Unique Bond Breaking in Crystalline Phase Change Materials and the Quest for Metavalent Bonding. *Advanced Materials* **30**, 1706735, (2018), doi:10.1002/adma.201706735.
- Kalb, J. A., Spaepen, F. & Wuttig, M. Kinetics of crystal nucleation in undercooled droplets of Sband Te-based alloys used for phase change recording. *Journal of Applied Physics* **98**, 054910, (2005), doi:10.1063/1.2037870.
- Raty, J.-Y., Schumacher, M., Golub, P., Deringer, V. L., Gatti, C. & Wuttig, M. A Quantum-Mechanical Map for Bonding and Properties in Solids. *Advanced Materials* **31**, 1806280, (2019), doi:10.1002/adma.201806280.
- Cheng, Y., Cojocaru-Mirédin, O., Keutgen, J., Yu, Y., Küpers, M., Schumacher, M., Golub, P., Raty, J.-Y., Dronskowski, R. & Wuttig, M. Understanding the Structure and Properties of Sesqui-Chalcogenides (i.e., V2VI3 or Pn2Ch3 (Pn = Pnictogen, Ch = Chalcogen) Compounds) from a Bonding Perspective. *Advanced Materials* **31**, 1904316, (2019), doi:https://doi.org/10.1002/adma.201904316.
- Maier, S., Steinberg, S., Cheng, Y., Schön, C.-F., Schumacher, M., Mazzarello, R., Golub, P., Nelson, R., Cojocaru-Mirédin, O., Raty, J.-Y. & Wuttig, M. Discovering Electron-Transfer-Driven Changes in Chemical Bonding in Lead Chalcogenides (PbX, where X = Te, Se, S, O). *Advanced Materials* 32, 2005533, (2020), doi:https://doi.org/10.1002/adma.202005533.
- Hegedüs, J. & Elliott, S. R. Microscopic origin of the fast crystallization ability of Ge–Sb–Te phase-change memory materials. *Nature Materials* **7**, 399-405, (2008), doi:10.1038/nmat2157.
- Matsunaga, T., Akola, J., Kohara, S., Honma, T., Kobayashi, K., Ikenaga, E., Jones, R. O., Yamada, N., Takata, M. & Kojima, R. From local structure to nanosecond recrystallization dynamics in AgInSbTe phase-change materials. *Nature Materials* **10**, 129-134, (2011), doi:10.1038/nmat2931.
- Raty, J. Y., Zhang, W., Luckas, J., Chen, C., Mazzarello, R., Bichara, C. & Wuttig, M. Aging mechanisms in amorphous phase-change materials. *Nat. Commun.* **6**, 7467, (2015), doi:10.1038/ncomms8467.